J. Chem. Thermodynamics 120 (2018) 106–115

Contents lists available at ScienceDirect

J. Chem. Thermodynamics

journal homepage: www.elsevier.com/locate/jct

Thermodynamic properties of $SrCl_2$(aq) from 252 K to 524 K and phase equilibria in the $SrCl_2$–H_2O system: Implications for thermochemical heat storage

Michael Steiger

University of Hamburg, Department of Chemistry, Germany

ARTICLE INFO

Article history:
Received 6 October 2017
Received in revised form 31 December 2017
Accepted 18 January 2018

Keywords:
Thermodynamics of $SrCl_2$(aq)
Pitzer ion interaction model
Dissociation of $SrCl_2$ hydrates
Solubility
Thermochemical heat storage

ABSTRACT

This paper reports a comprehensive thermodynamic treatment of the binary system $SrCl_2$–H_2O including solution properties and various phase equilibria. Published thermodynamic data of $SrCl_2$(aq), solubilities of the hydrates of strontium chloride and equilibrium data of the hydration–dehydration reactions have been collected and critically assessed. Using an internally consistent database of solution properties in the temperature range (252–524) K at 0.1 MPa or at saturation pressure (whichever is larger), the parameters of an ion interaction (Pitzer) model were determined. With this model, activity coefficients and water activities of saturated solutions of $SrCl_2$ hydrates were calculated yielding, together with equilibrium data of hydration–dehydration reactions, the thermodynamic solubility products of $SrCl_2{\cdot}6H_2O$, $SrCl_2{\cdot}2H_2O$ and $SrCl_2{\cdot}H_2O$. The complete phase diagram of the system $SrCl_2$–H_2O has been established and the potential use of $SrCl_2$ hydrates as thermochemical heat storage materials is discussed.

1. Introduction

There is a number of possible applications of salts and salt hydrates in the context of the storage or transformation of thermal energy. Such applications include the use in sorption processes [1–4], e.g. for dehumidification, desiccant cooling, drying, refrigeration or water recovery from the atmosphere, the use as phase change materials (PCM) [5–7] and for thermochemical heat storage [4,8,9]. Among other salts, the alkaline earth halides, in particular calcium and magnesium chloride, are suggested frequently for thermal energy applications. Generally, such applications are based on the release or absorption of heat during phase transformations or chemical reactions involving water vapor, the various hydrated forms of a salt and its aqueous solution. For example, strontium chloride is a possible candidate for thermochemical heat storage using the reversible dissociation of its various hydrates [9,10] and was suggested as an additive to calcium chloride in a mixed phase change material [11]. The prediction of the potential use and the behavior of a particular salt requires the knowledge of the complete phase diagram including vapor–liquid, solid–liquid and various solid–solid equilibria.

This paper focuses on the phase relations in the system $SrCl_2$–H_2O and their potential use for thermochemical heat storage. Strontium chloride forms a number of hydrates in the series $SrCl_2{\cdot}nH_2O$ including $SrCl_2{\cdot}6H_2O$, $SrCl_2{\cdot}2H_2O$, $SrCl_2{\cdot}H_2O$, $SrCl_2{\cdot}0.5H_2O$ and the anhydrous salt. The objective of this study was to use a thermodynamically consistent model to represent both the thermodynamic properties of $SrCl_2$(aq) and the solubility and hydration–dehydration equilibria in the $SrCl_2$–H_2O system. An appropriate set of equations for the representation of thermodynamic properties of aqueous electrolyte solutions is based on the Pitzer formalism [12]. The Pitzer equations incorporate an extended Debye–Hückel limiting law and a virial expansion representing short range ionic interactions. In its original form, only second and third virial coefficients are considered and the ionic strength dependence of the third virial coefficient is neglected. The original form of the model equations was used by Phutela et al. [13] to represent experimental heat capacities of $SrCl_2$(aq) to 373 K. They integrated their heat capacity equations to yield Gibbs energy data. However, their model extends to molalities of only 1 mol kg^{-1} and is not appropriate for the treatment of very concentrated solutions as required for solubility calculations.

For the treatment of very soluble electrolytes, several authors had to extend the original form of the equations including higher order terms with ionic strength dependence [14]. Holmes and Mesmer [15] reported on a more comprehensive treatment of the properties of $SrCl_2$(aq) to molalities of about 4 mol kg^{-1} and high temperatures up to 524 K. Even for this rather limited molality range, they had to use an extended form of the original equation.

E-mail address: michael.steiger@chemie.uni-hamburg.de

https://doi.org/10.1016/j.jct.2018.01.017
0021-9614/

Also Clegg et al. [16] had to use an extended Pitzer model equation including a fourth virial coefficient and the ionic strength dependence of the third virial coefficient to reproduce the available experimental data at 298.15 K to within the stated uncertainty. In the present work, we use the original version of the model, i.e. we neglect the ionic strength dependence of the third virial coefficient and we omit higher-order terms. However, we use an extension of the original equations that increases the numerical flexibility in the treatment of the ionic strength dependence of the second virial coefficient. This approach was also used in previous work with other highly soluble electrolytes [17–20]. The model for $SrCl_2$(aq) was used to calculate the activities in saturated solutions and to determine the thermodynamic solubility products which were then combined with hydration–dehydration equilibrium data to construct the complete phase diagram of the binary system including the stable and metastable phase boundaries involving $SrCl_2{\cdot}6H_2O$, $SrCl_2{\cdot}2H_2O$, $SrCl_2{\cdot}H_2O$ and anhydrous $SrCl_2$.

2. Theory and equations

The thermodynamic solubility product of a hydrate of composition $SrCl_2{\cdot}nH_2O$ is given by

$$\ln K_n = \ln(m_{Sr}/m^o) + 2\ln(m_{Cl}/m^o) + \ln\gamma_{Sr} + 2\ln\gamma_{Cl} + n\ln a_w \quad (1)$$

where m and γ are the saturation molalities and activity coefficients of Sr^{2+} and Cl^-, a_w is the water activity of the saturated solution and m^o = 1 mol kg^{-1}. In a binary $SrCl_2$ solution, this yields:

$$\ln K_n = 3\ln\left(4^{1/3} m/m^\circ\right) + 3\ln\gamma_\pm + n\ln a_w \quad (2)$$

where $\gamma_\pm$ is the mean activity coefficient. The water activity is related to the osmotic coefficient ϕ:

$$\ln a_w = -3m\phi/m_w \quad (3)$$

where m_w = 55.50844 mol·kg^{-1} is the molality of water. Neglecting the minor influence of the non-ideal behavior of water vapor, the water activity is also equal to the relative water vapor pressure $p_w/p_{w,0}$ where p_w and $p_{w,0}$ are the water vapor pressure and the water vapor saturation pressure. By definition, $\varphi = p_w/p_{w,0}$ where φ is the relative humidity (RH). The correction for the non-ideal behavior of water vapor is usually negligible except for the most accurate determinations of vapor pressure [21], hence, $a_w = \varphi$.

Additional phase equilibria include the dehydration (dissociation) reactions of the $SrCl_2$ hydrates:

$$SrCl_2 \cdot n_A H_2O(cr) \rightleftharpoons SrCl_2 \cdot n_B H_2O(cr) + (n_A - n_B)H_2O(g) \quad (4)$$

where subscripts A and B refer to two different hydrates containing n_A and n_B mol of water, respectively. The equilibrium constant of the dissociation reaction K_{AB} is given by

$$\ln K_{AB} = (n_A - n_B)\ln(p_{w,AB}/p^\circ) = (n_A - n_B)\ln(\varphi_{AB} p_{w,0}/p^\circ) \quad (5)$$

where p° = 0.1 MPa and $p_{w,AB}$ and φ_{AB} refer to the equilibrium water vapor partial pressure and the equilibrium relative humidity of the hydration–dehydration reaction, i.e. the dissociation humidity of a hydrate. The equilibrium constant K_{AB} and the dissociation humidity φ_{AB} are also related to the thermodynamic solubility products of the respective hydrates [22,23]:

$$\ln K_B = \ln K_A - (n_A - n_B)\ln\varphi_{AB} \quad (6)$$

Thus, the solubility product of a lower hydrated phase (with n_B mol H_2O) can be calculated from the solubility product of the hydrated phase (n_A mol H_2O) and the equilibrium humidity φ_{AB} of the dissociation equilibrium.

In order to represent the available thermodynamic data for $SrCl_2$(aq) and to calculate the activities of water and dissolved ions the original version of the Pitzer ion interaction approach [12] was used, i.e. the ionic strength dependence of the third virial coefficient was neglected and higher-order terms were omitted. However, an extended form of the original equations to increase the numerical flexibility at very high concentration by including the parameter $\beta^{(2)}_{MX}$ was used. In the original Pitzer equations, this parameter was introduced for the treatment of 2-2 electrolytes to avoid the explicit calculation of association equilibria [12]. In our earlier work, the use of $\beta^{(2)}_{MX}$ together with an appropriate value of the exponential coefficient α_2 proved to be helpful to represent activities to very high ionic strength [17–20].

The virial coefficients are empirical quantities which are evaluated from experimental osmotic and activity coefficients. The adjustable parameters are the binary interaction parameters ($\beta^{(0)}_{MX}$, $\beta^{(1)}_{MX}$, $\beta^{(2)}_{MX}$, C^{ϕ}_{MX}). The temperature dependence of the interaction parameters is obtained from experimental data at different temperatures and is expressed by

$$P(T) = q_1 + q_2(1/T - 1/T_R)T_0 + q_3\ln(T/T_R) + q_4(T - T_R)/T_0 + q_5(T^2 - T_R^2)/T_0^2 \quad (7)$$

Here, T_0 = 1 K and the reference temperature is T_R = 298.15 K. In addition to osmotic and activity coefficients, there is also interest in enthalpies and heat capacities of electrolyte solutions which also yield the temperature dependence of the interaction parameters. The Pitzer equations also include appropriate expressions for the apparent relative molar enthalpy, ${}^{\phi}L$, and the apparent molar heat capacity, ${}^{\phi}C_p$ [12]. The apparent molar heat capacity is defined as:

$${}^{\phi}C_p = (C_p - n_w C_p^\circ)/n_s \quad (8)$$

where C_p is the total heat capacity of the solution, C_p° is the molar heat capacity of pure water, and n_w and n_s are the number of moles of water and solute, respectively. The partial molar heat capacity at infinite dilution, ${}^{\phi}C_p^\circ$, is treated as an adjustable parameter and is represented by:

$${}^{\phi}C_p^\circ = p_1 + p_2 T + p_3/T \quad (9)$$

Experimental data suitable for the determination of ${}^{\phi}L$ are heats of dilution and integral heats of solution. The enthalpy change on diluting a solution from molality m_1 to molality m_2 yields $\Delta^{\phi}L = {}^{\phi}L_2 - {}^{\phi}L_1$. The integral heat of solution per mole of solute, $\Delta_{sol}H$, is related to ${}^{\phi}L$ through the enthalpy of solution per mole of solute at infinite dilution, $\Delta_{sol}H^\circ$, by

$$\Delta_{sol}H = \Delta_{sol}H + {}^{\phi}L \quad (10)$$

3. Results and discussion

3.1. Determination of model parameters

The data used for the determination of the ion interaction parameters for $SrCl_2$(aq) are listed in Table 1. There are several studies that report isopiestic vapor pressure data for $SrCl_2$(aq) at 298.15 K [16,24–29]. The isopiestic reference electrolytes used in these studies were KCl [24,26], NaCl [16,27,29] and $CaCl_2$ [25,28]. All osmotic coefficients of $SrCl_2$(aq) were recalculated using the equations of Archer for NaCl(aq) [30] and KCl(aq) [31] and of Rard and Clegg for $CaCl_2$(aq) [32]. Following the previous critical evaluations [16,28], the data of Stokes [25], Downes [26], Macaskill et al. [27], Rard and Miller [28] and Clegg et al. [16] were given full weight in the subsequent data treatment. Also, most of the recent data reported by Guo et al. [29] agree very well with the remaining data at 298.15 K and were included in the final fit. Holmes and Mesmer [15,33] provided two very comprehensive sets of data using NaCl(aq) as the reference electrolyte at high temperatures

Table 1
Literature sources for activity and thermal properties of $SrCl_2$(aq).

Property[a]	T/K	m/mol kg^{-1}	N[b]	σ_{est}[c]	σ_{fit}[c]	Reference
ϕ(isop.)	298.15	0.12–2.6	0 (20)	0.02	0.024	[24]
ϕ(isop.)	298.15	0.08–4.0	20 (20)	0.005	0.008	[25]
ϕ(isop.)	298.15	0.35–2.2	18 (18)	0.002	0.005	[26]
ϕ(isop.)	298.15	0.7–3.1	14 (14)	0.002	0.005	[27]
ϕ(isop.)	298.15	2.7–3.8	29 (29)	0.002	0.002	[28]
ϕ(isop.)	298.15	1.7–2.0	4 (4)	0.002	0.007	[16]
ϕ(isop.)	298.15	0.2–3.5	25 (27)	0.004	0.007	[29]
ϕ(isop.)	383–474	0.47–4.2	157 (158)	0.005	0.007	[33]
ϕ(isop.)	383–473	0.41–5.5	144 (148)	0.005	0.005	[15]
ϕ(v.p.)	298.15	0.2–3.5	0 (11)	0.05	0.051	[34]
ϕ(v.p.)	303–343	0.66–3.2	0 (40)	0.05	0.095	[35]
ϕ(f.t.)	260.2–271.4	0.36–1.8	5 (7)	0.05	0.027	[36]
ϕ(f.t.)	265.2–270.1	0.57–1.3	0 (3)	0.05	0.050	[37]
ϕ(f.t.)	270.6–273.1	0.01–0.5	6 (6)	0.05	0.017	[38]
ϕ(f.t.)	256.7–267.1	1.0–2.1	3 (3)	0.05	0.061	[39]
ϕ(f.t.)	267.2–273.1	0.01–1.02	8 (10)	0.05	0.027	[40]
ϕ(f.t.)	265.3–272.4	0.15–1.27	8 (8)	0.05	0.039	[41]
ϕ(f.t.)	270.5–272.7	0.1–0.5	3 (3)	0.05	0.032	[42]
ϕ(f.t.)	258.2–265.2	1.3–2.20	1 (3)	0.05	0.004	[43]
ϕ(b.t.)	374–391	0.7–7.4	0 (35)	0.2	0.175	[45]
ϕ(b.t.)	373.3–374.8	0.12–1.1	0 (5)	0.02	0.014	[46]
ln$\gamma_\pm$ (emf)	298.15	0.01–3.0	0 (9)	0.02	0.031	[48]
ln$\gamma_\pm$ (emf)	283–343	0.0001–0.03	0 (179)	0.02	0.021	[49]
ln$\gamma_\pm$ (diff)	298.15	0.0001–0.01	7 (7)	0.003	0.0046	[50]
ln$\gamma_\pm$ (calc)	298.15	0.001–4.0	32 (32)	0.003	0.0049	[16]
$^{\phi}L(\Delta_{dil}H)$	273–307	0.06–2.2	0 (65)[d]	0.25	0.01–2	[51]
$^{\phi}L(\Delta_{dil}H)$	298.15	0.2–3.2	0 (27)	0.2	0.344	[52]
$^{\phi}L(\Delta_{dil}H)$	298.15	0.003–0.1	9 (9)	0.01	0.013	[53]
$^{\phi}L(\Delta_{dil}H)$	303.15	0.23–1.0	6 (6)	0.02	0.020	[54]
$^{\phi}L(\Delta_{sol}H)$	273–338	0.0001–3.5	65 (91)	0.5	0.71	[55]
$^{\phi}C_p$	298.15	0.30–1.0	4 (6)	0.015	0.013	[56]
$^{\phi}C_p$	298.15	0.14–2.8	6 (10)	0.015	0.045	[57]
$^{\phi}C_p$	298.15	0.013–0.33	8 (8)	0.005	0.030	[58,59]
$^{\phi}C_p$	298.15–372.15	0.05–1.05	20 (20)	0.005	0.013	[60]

[a] Quantity and experimental technique (isop.: isopiestic; v.p.: vapor pressure; f.t.: freezing temperature; b.t.: boiling temperature; emf: electrochemical cell potentials; diff: diffusion measurements; calc: calculated by Ref. [16]).
[b] Number of data used in fit (total number of measurements in brackets).
[c] The units of the standard errors σ_{est} and σ_{fit} are kJ·mol^{-1} for $^{\phi}L$ and kJ·mol^{-1}·K^{-1} for $^{\phi}C_p$.
[d] values digitized from Plate I in reference[51].

(383 K to 524 K). Their data, after recalculation were also given full weight in the further data treatment.

Direct vapor pressure measurements reported by Hepburn [34] at 298.15 K and by Patil et al. [35] at (303–343) K are significantly scattered and show systematic deviations from the isopiestic data, thus, they were not considered further. Freezing point measurements [36–43] provide additional data at low temperatures. Osmotic coefficients were calculated from the freezing temperatures using the equation of Klotz and Rosenberg [44]. Most of the data show significant scatter. Nonetheless, most freezing temperatures were included in the database with reduced weight in order to guide the fit at low temperatures. The only available boiling temperatures of $SrCl_2$ solutions are the very old data tabulated in the compilation of Timmermans [45]. Most of these data are not compatible with the high quality isopiestic data [15,33] and show large systematic deviations. The only exception are the data of Baroni [46].

As noted by several authors [15,16,28,47], the available measurements of electrochemical cell potentials [48,49] are seriously in error and were, therefore, not included in the data treatment. The only source of activity coefficients at low molalities are diffusion measurements [50] which are consistent with the treatment of Clegg et al. [16] and their tabulated activity coefficients. Both datasets, the activity coefficients of Harned [50] and the smoothed values of Clegg et al. [16] at 298.15 K that were calculated with their extended isothermal model were included in the final database for the determination of the model parameters.

Available thermal data include heats of dilution [51–54] at (273–307) K, heats of solution [55] at (273–338) K and heat capacities [56–60] at (298.15–373.15) K. The heats of dilution of Pratt [51] and of Stearn [52] are not compatible with the remaining data and show significant systematic deviations. In contrast, the heats of dilution of both Lange and Streeck at 298.15 [53] and Leung and Millero at 303.15 K [54] are fully consistent with the remaining data and were given full weight. The heats of solution of Mishchenko and Stagis [55] at low concentrations show significant scatter and are not compatible with the remaining data at low temperature (below 298.15 K). While their measurements at higher concentrations were given full weight in the final treatment, their measurements at low concentrations (<0.3 mol kg^{-1}) were included with reduced weight only. Also, their values of the enthalpy of solution at infinite dilution, $\Delta_{sol}H^{\circ}$, were accepted.

Apparent molar heat capacities were calculated using Eq. (8) with the values for pure water taken from Wagner and Pruß [61]. Using different values for pure water, e.g. those of Kell [62] that were used in many earlier studies, resulted in large differences in the calculated apparent molar heat capacities at low molalities. As noted earlier [63], these deviations at the lowest molalities lead to different values of the apparent molar heat capacities of the solute at infinite dilution ($^{\phi}C_p^{o}$) which are no longer consistent with recommended values of $^{\phi}C_p^{o}$ [64] that are based on older data using different heat capacities of pure water.

The available heat capacities at 298.15 K are in reasonable agreement with each other. The measurements of Perron et al.

[58] with a flow calorimeter and the subsequent corrections of their data reported by Desnoyers et al. [59] are the most important source of data at low molalities. Though more scattered, also the earlier measurements with batch calorimeters [56,57] are consistent with their data. The only available data at temperatures different from 298.15 K are those of Saluja and LeBlanc [60]. Their measurements were made at 0.6 MPa and cover the temperature range from (298–373) K and the molality range (0.2–1) mol kg^{-1}. The influence of pressure on the ion interaction parameters is not considered in the present study and it is assumed that such a small deviation has only a negligible influence. Nonetheless, for the calculation of the apparent molar heat capacities from the data of Saluja and LeBlanc the values for pure water at 0.6 MPa from Wagner and Pruβ [61] were used. The data of Saluja and LeBlanc [60] were also found to be consistent with the remaining data. Therefore, with the exception of a few outliers (see Table 1) most of the heat capacity data were included in the least squares treatment.

The database listed in Table 1 covers the temperature range (258–524) K. The upper molality limit is 5.5 mol kg^{-1} which is about the solubility of $SrCl_2·6H_2O$ near 334 K, i.e. close to the $SrCl_2·6H_2O$–$SrCl_2·2H_2O$ decomposition temperature. However, at higher temperatures, the solubility of the respective stable hydrates $SrCl_2·2H_2O$ and $SrCl_2·H_2O$ increases rapidly reaching values >10 mol kg^{-1} above 473 K. Therefore, to improve the database at high temperature, additional vapor pressure data of saturated solutions were also evaluated (cf. Table 2). Usually, the water activities of saturated solutions, i.e. the deliquescence humidities (DRH) of the respective solid phases, are not used in the determination of ion interaction parameters as such data show typically larger scatter and systematic deviations [20]. Therefore, in the present study, only those data were used that helped to fill the gaps in the available database at high temperature and molality. There is a number of studies reporting vapor pressures $p_{w,sat}$ of saturated solutions [65–74], however, only one study [67] reports saturation vapor pressures of $SrCl_2·2H_2O$ at high temperatures (see Table 2). Osmotic coefficients were calculated from the saturation vapor pressures of Collins and Menzies [67] using the saturation molalities at the respective temperatures from the available solubility data by interpolation. With these data, the upper molality limit was shifted to 7.8 mol kg^{-1} which corresponds to the solubility of $SrCl_2·2H_2O$ at 400 K. To guide the fit at even higher molalities, estimated values of ϕ in the supersaturated region were included in the fit (cf. Fig. 1) in order to eliminate unfavorable extrapolation behavior and to guarantee a smooth extrapolation of the water activity isotherms at 383 K, 473 K, 498 K and 524 K.

The final database for $SrCl_2$(aq) then covers the temperature range (258–524) K to saturation molality at 0.1 MPa or at saturation pressure. The estimated standard errors listed in column 5 of Table 1 were used to weight the different types of data in the least squares treatment. Error estimates are based on reported experimental errors, internal consistency and scatter of each dataset and on the compatibility with the remaining data. All data were included in a simultaneous least squares fit to the ion interaction equations for ϕ, $\ln\gamma$, ${}^{\phi}L$ and ${}^{\phi}C_p$ to determine the parameters of Eq. (7). In addition to the weighting scheme using the estimated absolute standard errors listed in Table 1, relative weights were assigned to the different property data (i.e. osmotic and activity coefficients, heats of dilutions and apparent molar heat capacities) that have numerical values differing by orders of magnitude. This was to make sure that the different types of data enter with comparable weight in the least squares fit.

Values of the Debye-Hückel parameters A_L and A_J were taken from Archer and Wang [75]. Values of A_ϕ are also based on Archer and Wang but the simpler expression for A_ϕ given in reference [76] was used which is valid at 0.1 MPa and saturation pressure and to 473 K. This leads to minor deviations above 473 K where extrapolation is required. For consistency, the present model equations should be used with the equation for A_ϕ given in reference [76].

As mentioned before, the quality of the fit was not satisfactory when the conventional three parameter Pitzer equations with the parameters $\beta^{(0)}_{MX}$, $\beta^{(1)}_{MX}$ and C^{ϕ}_{MX} were used. Therefore, the additional parameter $\beta^{(2)}_{MX}$ used in our previous studies [17–20] was also used here. Values of $\alpha_1 = 1.7$ $kg^{1/2}$ $mol^{-1/2}$ and $\alpha_2 = 0.1$ $kg^{1/2}$ $mol^{-1/2}$ were fixed after trial calculations. The final model parameters are listed in Table 3 and the standard errors of the fit are summarized in column 6 of Table 1. Osmotic coefficients are shown in Fig. 1a. The lines represent calculated values plotted as isotherms at 298.15 K, 382.96 K, 413.36 K, 443.92 K, 473.61 K, 498.5 K and 523.66 K. Symbols represent the isopiestic data at the same temperatures. There is very good agreement in all cases and the course of the calculated isotherms at high concentrations, where no experimental data are available, seems to be reasonable. The data used to guide the fit in this concentration range are the vapor pressures of saturated solutions of $SrCl_2·2H_2O$ reported by Collins and Menzies [67] (white squares in Fig. 1a) and estimated osmotic

Table 2
Literature sources for vapor pressures of saturated solutions of $SrCl_2·6H_2O$, $SrCl_2·2H_2O$ and $SrCl_2·H_2O$.

T/K	N[(b)]	$\sigma_{fit}(\phi)$	$\sigma_{fit}(a_w)$	Reference
$SrCl_2·6H_2O$				
293.15[(a)]	0 (1)	0.556	0.0694	[66]
303.15–333.15	0 (4)	0.034	0.0052	[67]
298.15	0 (1)	0.012	0.0017	[68]
278.15–313.15	0 (8)	0.077	0.0105	[69]
278.15–303.15	0 (6)	0.022	0.0027	[70]
298.15	0 (1)	0.015	0.0020	[71]
293.15–343.15	0 (11)	0.058	0.0094	[72]
298.15	0 (1)	0.015	0.0020	[73]
254–283.15	0 (5)	0.136	0.0077	[74]
$SrCl_2·2H_2O$				
353.15–373.15	0 (2)	0.046	0.0081	[65]
338.15–403.15	5 (7)	0.021	0.0041	[67]
298.15–343.15	0 (8)	0.048	0.0077	[72]
$SrCl_2·H_2O$[(b)]				
338.15–363.15	0 (4)	0.082	0.0109	[72]

[(a)] This value is an obvious outlier and is not shown in Fig. 4
[(b)] Due to problems in the determination of its exact water content, this solid is reported as $SrCl_2·xH_2O$ in reference [72].

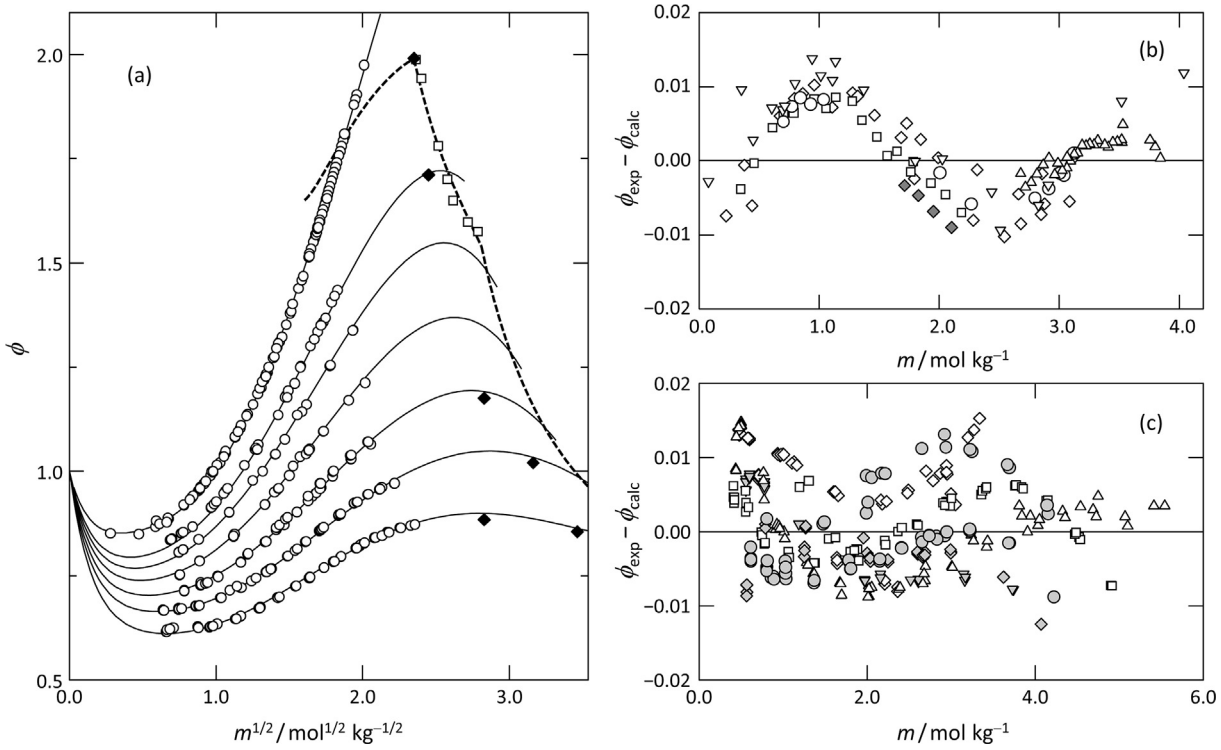

Fig. 1. (a) Osmotic coefficients ϕ against square root of molality ($m^{1/2}$) at 298 K, 383 K, 413 K, 444 K, 474 K, 499 K and 524 K (from top to bottom); circles: isopiestic data [15,16,25–29,33], squares: vapor pressure measurements of solutions saturated with $SrCl_2{\cdot}2H_2O$ [67]; diamonds: estimated values used in least squares fit; solid curves calculated with parameters from Table 3; dashed curves solutions saturated with $SrCl_2{\cdot}6H_2O$, $SrCl_2{\cdot}2H_2O$ and $SrCl_2{\cdot}H_2O$. (b) Deviations of the calculated osmotic coefficients from experimental data at 298.15 K [16,25–29]. (c) Deviations of the calculated osmotic coefficients from experimental data [15,33] at the other temperatures.

Table 3
Parameters of Eqs. (7) and (9) for the temperature dependence of the model parameters for $SrCl_2$(aq).

Parameter	Value	Parameter	Value	Parameter	Value
$\beta^{(0)}_{MX}$		$\beta^{(1)}_{MX}$		$\beta^{(2)}_{MX}$	
q_1/kg mol^{-1}	1.35306E+00	q_1/kg mol^{-1}	1.75011E+00	q_1/kg mol^{-1}	−1.27132E+00
q_2/kg mol^{-1}	5.81463E+03	q_2/kg mol^{-1}	−9.07152E+04	q_2/kg mol^{-1}	0
q_3/kg mol^{-1}	7.64534E+01	q_3/kg mol^{-1}	−7.00314E+02	q_3/kg mol^{-1}	−3.23881E+01
q_4/kg mol^{-1}	−2.82906E−01	q_4/kg mol^{-1}	1.76013E+00	q_4/kg mol^{-1}	1.75760E−01
q_5/kg mol^{-1}	1.46843E−04	q_5/kg mol^{-1}	−7.19941E−04	q_5/kg mol^{-1}	−1.03353E−04
C^{ϕ}_{MX}		${}^{\phi}C^{\circ}_{p}$			
q_1//kg^2 mol^{-2}	−3.21710E−02	p_1/J mol^{-1} K^{-1}	6.75724E+03	α_1/kg$^{1/2}$ mol$^{-1/2}$	1.7
q_2//kg^2 mol^{-2}	0	p_2/J mol^{-1} K^{-2}	−4.80908E+00	α_2/kg$^{1/2}$ mol$^{-1/2}$	0.1
q_3//kg^2 mol^{-2}	−1.55844E+00	p_3/J mol^{-1}	−1.27480E+06		
q_4//kg^2 mol^{-2}	7.79261E−03				
q_5//kg^2 mol^{-2}	−4.54178E−06				

coefficients at (474–524) K and high molalities (diamonds) which were obtained by graphical extrapolation of plots of water activities against molality.

Upon closer inspection of the residuals shown in Fig. 1b and c, a cyclic deviation of the calculated values from the experimental data is obvious indicating that a greater number of parameters might do better. In fact, Clegg et al. [16] had to use a five parameter extended Pitzer equation to represent the data at 298.15 K essentially within the experimental uncertainties. As the present model covers a broad range of temperatures and is valid to significantly higher molalities, the agreement between the experimental data and the calculations with the present four parameter model is considered very satisfactory (Fig. 1b and 1c and root mean square errors in Table 1). The root mean square deviations of the present model and the isothermal equation of Clegg et al. [16] are 0.004 and 0.005 for ϕ and $\ln\gamma_{\pm}$, respectively.

There is also very good agreement between the model calculated heats of dilution with the available experimental data at 298.15 K [53] and 303.15 K [54]. Most likely, the deviations do not exceed the experimental uncertainties. In the case of the apparent molar heat capacities, the standard error of the fit only slightly exceeds the expected experimental uncertainty of the data reported in references [58–60]. The quality of the available experimental data at low temperatures is less satisfactory. Nonetheless, the model reproduces the available freezing temperatures [36–43] to within the stated uncertainty.

3.2. Solubility products of $SrCl_2{\cdot}nH_2O$

According to Eqs. (2) and (6), both solubility data and equilibrium relative humidities are suitable for the calculation of the thermodynamic solubility products of the various hydrates. Tables 4 and 5 list a collection of literature sources of solubility data [25,28,43,72,77–91] and equilibrium relative humidities [66,67,92–97] for the decomposition reactions of the hydrates. Consistent solubilities are shown in Fig. 2 together with selected

Table 4
Sources of solubility data in the system $SrCl_2$–H_2O.

T/K	N[a]	Reference	T/K	N[a]	Reference
$SrCl_2·6H_2O$					
272.65–330.15	0 (6)	[77]	273.15–330.65	0 (11)	[78]
273.15–313.15	0 (2)	[79]	256.15–332.15	0 (13)	[80]
298.15	1 (1)	[81]	296.05–334.05	5 (5)	[82]
278.65–288.25	2 (2)	[83]	298.15–323.15	0 (2)	[84]
298.15	1 (1)	[25]	291.15–334.45	6 (6)	[86]
291.15–333.15	5 (5)	[87]	313.15–343.35	2 (2)	[72]
298.15	1 (1)	[28]	258.15–298.15	5 (5)	[43]
291.30–334.32	0 (5)	[88]	298.15	1 (1)	[89]
323.15	1 (1)	[90]			
$SrCl_2·2H_2O$					
340.15–379.15	0 (4)	[77]	338.15–391.95	0 (8)	[78]
337.15–417.15	0 (11)	[80]	336.1–407.55	6 (6)	[82]
397.15–428.15	0 (6)	[85]	334.45	1 (1)	[86]
373.15	1 (1)	[87]	313.15	0 (1)	[72]
335.55–387.40	0 (7)	[88]	348.15	1 (1)	[91]
$SrCl_2·H_2O$					
426.15–523.15	2 (5)	[80]	407.55–465.75	9 (9)	[82]
457.15–691.15	1 (7)	[85]	343.35–353.15	0 (2)	[72][b]

[a] Number of data used in least squares fit (total number of experimental data).
[b] Due to problems in the determination of its exact water content, this solid is reported as $SrCl_2·xH_2O$ in reference [72].

Table 5
Sources of dissociation equilibrium humidities in the system $SrCl_2$–H_2O.

T/K	N[a]	Reference	T/K	N[a]	Reference
$SrCl_2·2H_2O$–$SrCl_2·6H_2O$					
290.05–328.65	0 (14)	[92]	287.90–312.60	0 (6)	[93]
278.15–313.15	0 (6)	[94]	273.15–298.15	2 (3)	[95]
283.85–308.40	0 (8)	[96]	293.15–298.15	1 (2)	[66]
298.15–333.15	8 (8)	[67]	298.15–313.15	0 (4)	[97]
$SrCl_2·2H_2O$–$SrCl_2·H_2O$					
293.15–373.15	0 (4)	[94]	308.15–336.95	0 (5)	[96]
298.15–403.15	16 (16)	[67]			
$SrCl_2·H_2O$–$SrCl_2$					
355.65–375.15	5 (5)	[96]			

[a] Number of data used in least squares fit (total number of experimental data).

freezing and boiling temperatures (cf. Table 1). Most of the available solubilities of $SrCl_2·6H_2O$ provide a consistent database. Several data, mainly very old measurements, show larger scatter or systematic deviations [77–80,84,88] and were not included in the further evaluation. The remaining data [25,28,43,72,81–83,86,87,89,90] were used to calculate values of the thermodynamic solubility product of $SrCl_2·6H_2O$ using Eq. (2) and the model calculated activities. The resulting values of $\ln K_6$ are depicted in Fig. 3a (the rejected data are not shown). Their temperature dependence was represented by a fit to Eq. (7) yielding the coefficients listed in Table 6. The calculated solubility products are also shown in Fig. 3.

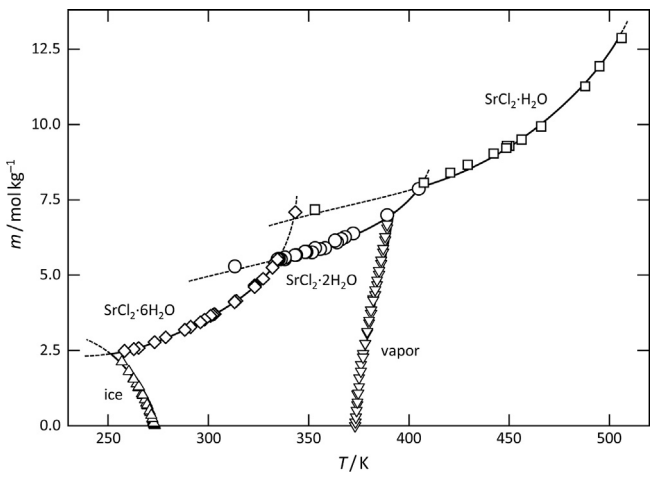

Fig. 2. Freezing temperatures, boiling temperatures and solubilities in the system $SrCl_2$–H_2O (at 0.1 MPa or at saturation pressure, whichever is larger). Symbols represent critically evaluated experimental data; solid curves represent model calculated freezing and boiling temperatures and the stable solubilities of $SrCl_2·6H_2O$, $SrCl_2·2H_2O$ and $SrCl_2·H_2O$; dashed lines are calculated metastable equilibria.

According to Eq. (6), the solubility products $\ln K_6$ were then used together with the available dissociation relative humidities (listed in Table 5) to calculate values of the thermodynamic solubility product $\ln K_2$ of $SrCl_2·2H_2O$ which were combined with the values of $\ln K_2$ obtained from solubilities of $SrCl_2·2H_2O$ together with the ion interaction model. The available solubility data show significant scatter. Only the data of Menzies [82], Assarsson [86,87] and Li et al. [91] were found to be consistent both with each other and with the dissociation humidities reported by Diesnis [66], Collins and Menzies [67] and Baxter and Lansing [95]. The remaining decomposition humidities of the hexahydrate [92–94,96,97] are systematically low and were rejected. The remaining solubility data [77,78,80,85,88] show larger scatter or deviations and were not considered. The metastable solubility of $SrCl_2·2H_2O$ at 313.15 K reported in reference [72] (white circle in Fig. 2, white diamond in Fig. 3b) is also not fully consistent with the dissociation humidities. The final data base of $\ln K_2$ values is shown in Fig. 3b yielding the parameters of Eq. (7) for $SrCl_2·2H_2O$ listed in Table 6.

The database of solubilities of $SrCl_2·H_2O$ is sparse. The most reliable data are those of Menzies [82] while the other data show

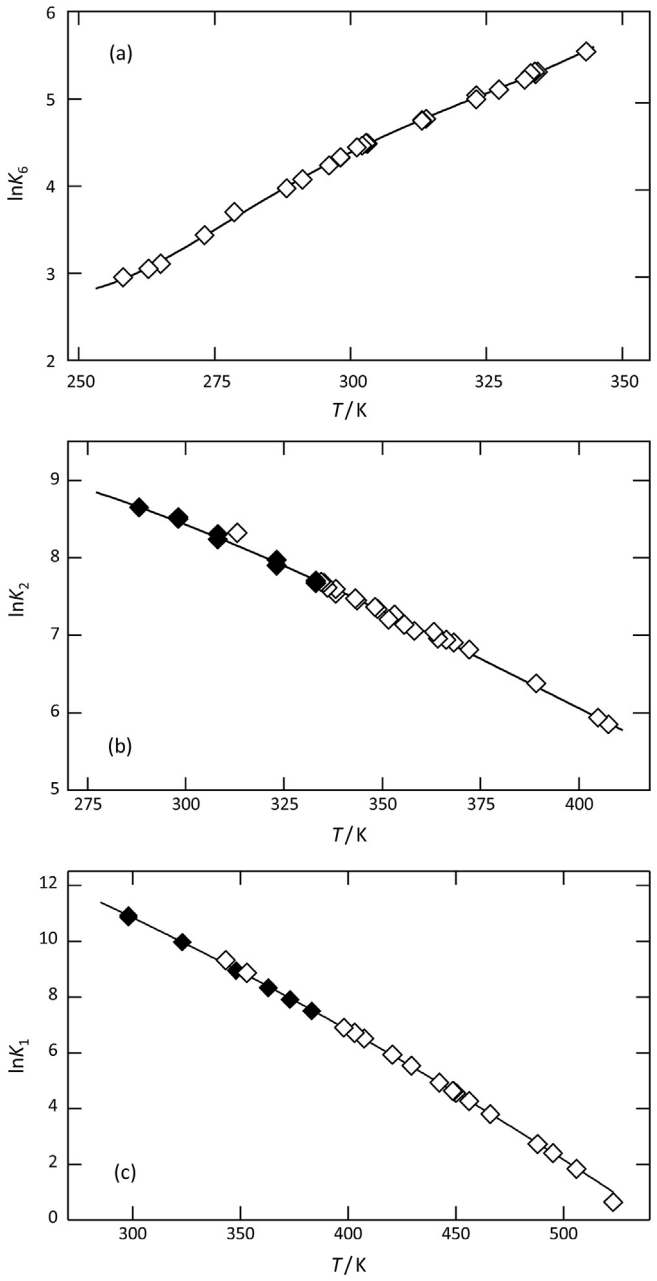

Fig. 3. Thermodynamic solubility products of $SrCl_2·6H_2O$ (a), $SrCl_2·2H_2O$ (b) and $SrCl_2·H_2O$ (c) calculated from solubilities (white symbols) and from dissociation equilibrium humidities (black symbols).

significant scatter. Only two values of Etard [80] and one of Benrath [85] at very high temperatures were consistent with the data of Menzies [82] and were included in the data treatment. Again, the two metastable solubilities at low temperature reported by Bergthorsson [72] are not fully consistent with the dissociation humidities of the dihydrate and seem to be slightly high (Figs. 2 and 3b). The solubility products $\ln K_1$ calculated from the dissociation humidities for the $SrCl_2·2H_2O$–$SrCl_2·H_2O$ transition reported by Collins and Menzies [67] agree nicely with the solubility products calculated from the solubilities of the monohydrate and form a consistent database (Fig. 3c). In contrast, the remaining dissociation humidities [94,96] are systematically low and were rejected. The data shown in Fig. 3c yield the coefficients of Eq. (7) for $SrCl_2·H_2O$ listed in Table 6.

Not much is known about phases with lower water content than the monohydrate. The existence of the hemihydrate $SrCl_2·0.5H_2O$ was postulated [98,99] and the compound was successfully prepared by Lutz et al. [100]. However, no solubilities or other thermodynamic data are available for this solid. Therefore, a clear statement about its stable existence in the $SrCl_2$–H_2O system is hardly possible. Kessis [98] claimed, based on DSC measurements, that the hemihydrate is the stable solid in contact with a saturated solution between 522 K and 611 K. The only experimental solubility data at high temperature are those of Benrath [85] covering the temperature range (397–685) K. At lower temperatures, these data are quite scattered and were not used for the determination of the solubility products of $SrCl_2·2H_2O$. Benrath [85] claims transition temperatures for the $SrCl_2·2H_2O$–$SrCl_2·H_2O$ and $SrCl_2·H_2O$–$SrCl_2$ transitions at 503 K and 593 K, respectively. He did not observe the hemihydrate. Therefore, the question whether the hemihydrate occurs as a stable solid is considered unresolved and requires additional experimental data. Since the present model for $SrCl_2$(aq) is limited to about 523 K and in lack of reliable data, the hemihydrate was not considered in the present treatment.

3.3. The phase diagram $SrCl_2$–H_2O

Using the present ion interaction model together with the thermodynamic solubility products, all relevant phase equilibria involving $SrCl_2·6H_2O$, $SrCl_2·2H_2O$ and $SrCl_2·H_2O$ can be calculated, i.e. freezing and boiling temperatures, solubilities and hydration–dehydration phase boundaries. Calculated solubilities, freezing temperatures and boiling temperatures are compared to experimental data in Fig. 2. There is excellent agreement also on the metastable branches where experimental data are available. The complete humidity–temperature phase diagram of the $SrCl_2$–H_2O system is shown in Fig. 4. In this representation, solid–liquid equilibria are represented by the water activities of the saturated solutions ($a_{w,sat} = \varphi_{sat}$), i.e. the deliquescence humidities of the respective crystalline phases. There is very good agreement between the model calculated $a_{w,sat}$ of $SrCl_2·6H_2O$, $SrCl_2·2H_2O$ and $SrCl_2·H_2O$ and the most reliable experimental data [24,65,67,70–73] (see also Table 2). It should be noted that most of these data were not used in the determination of the model parameters. The calculated dissociation equilibrium humidities (for the $SrCl_2·6H_2O$–$SrCl_2·2H_2O$ and the $SrCl_2·2H_2O$–$SrCl_2·H_2O$ phase boundaries (φ_{AB}) also agree nicely with experimental data. Deviations do not exceed the expected experimental errors which is confirmed by the root mean square (*rms*) deviations of $\sigma_{rms}(\varphi) = 0.0058$ and $\sigma_{rms}(\varphi) = 0.0094$, respectively.

The invariant points of the system $SrCl_2$–H_2O are the intersections of the monovariant curves in Fig. 4. Invariant points obtained in this study are listed in Table 7. The invariant point ice + $SrCl_2·6H_2O$ + solution + vapor is modeled at 251.2 K and the boiling temperature of the saturated solution is 392.2 K. The stable

Table 6
Parameters of Eq. (7) for the temperature dependence of the thermodynamic solubility products.

Solid	q_1	q_2	q_3	q_4	q_5
$SrCl_2·6H_2O$	4.32637E+00	6.26145E+05	6.29195E+03	−2.09173E+01	1.15543E−02
$SrCl_2·2H_2O$	8.46396E+00	−5.13755E+03	−2.31076E+01	0	0
$SrCl_2·H_2O$	1.09108E+01	3.67868E+03	2.86389E+01	−9.20418E−02	0

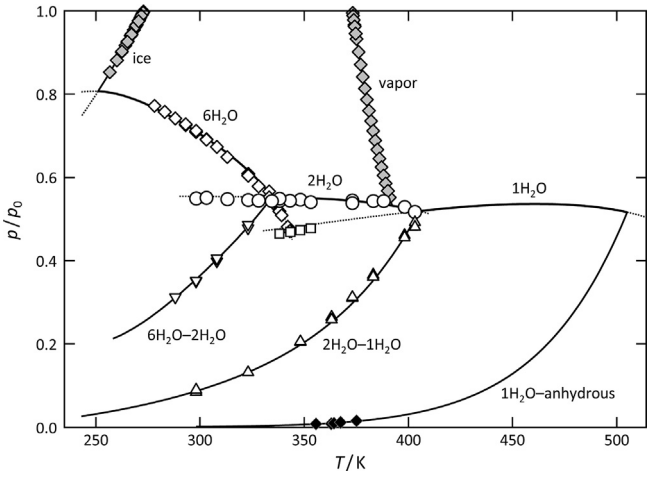

Fig. 4. Humidity–temperature phase diagram of the $SrCl_2$–H_2O system (at 0.1 MPa or saturation pressure, whichever is larger). Symbols represent critically evaluated experimental data and have the following meaning: $SrCl_2{\cdot}6H_2O$–$SrCl_2{\cdot}2H_2O$ equilibrium ($6H_2O$–$2H_2O$, inverted triangles), $SrCl_2{\cdot}2H_2O$–$SrCl_2{\cdot}H_2O$ equilibrium ($2H_2O$–$1H_2O$, triangles), $SrCl_2{\cdot}H_2O$–$SrCl_2$ equilibrium ($1H_2O$–anhydrous, black diamonds), boiling and freezing temperatures (gray diamonds) and the deliquescence humidities of hexahydrate ($6H_2O$: white diamonds), dihydrate ($2H_2O$: circles) and monohydrate ($1H_2O$: squares); solid lines are calculated freezing and boiling temperatures, deliquescence and dissociation humidities, dotted lines represent metastable equilibria.

existence of the hexahydrate is limited by the invariant point $SrCl_2{\cdot}6H_2O$ + $SrCl_2{\cdot}2H_2O$ + solution + vapor which is modeled at 334.6 K in excellent agreement with the careful experimental determination of the transition temperature that gave 334.5 K [101]. The invariant point $SrCl_2{\cdot}2H_2O$ + $SrCl_2{\cdot}H_2O$ + solution + vapor is modeled at 405.3 K. This value is somewhat lower than the transition temperature of 407.6 K solely derived from solubility measurements by Menzies [82] but is in very good agreement with the value reported by Collins and Menzies [67] based on their measurements of dissociation pressures and vapor pressure of saturated solutions. The deviations are largely the result of a minor inconsistency between solubility and dissociation pressure data.

According to Lutz et al. [100], $SrCl_2{\cdot}0.5H_2O$ only forms above about 438 K. Thus, the dehydration of the monohydrate at low temperature directly yields the anhydrous salt. Dissociation humidities for this transition at (355–375 K) are available [96]. However, the reliability of these data is uncertain as data reported by the same authors for the dissociation humidities of the hexahydrate and the dihydrate, respectively, are systematically low. Nonetheless, these data were combined with the solubilities reported by Benrath [85] at 506.15 K and 538.15 K to assess the solubility product of anhydrous $SrCl_2$, i.e. neglecting the hemihydrate. These solubility products were then used to estimate the equilibrium humidities of the $SrCl_2{\cdot}H_2O$–$SrCl_2$ transition at high temperatures. This treatment yields the following expression for the equilibrium humidity φ_{1-0} of the $SrCl_2{\cdot}H_2O$–$SrCl_2$ phase boundary:

$$\ln \varphi_{1-0} = q_1 + q_2(1/T - 1/T_R)T_0 + q_3 \ln(T/T_R) \quad (11)$$

Table 7
Invariant points in the system $SrCl_2$–H_2O.

Phase assemblage	T/K	m/mol·kg^{-1}	$\varphi = a_w$
ice + $6H_2O$ + solution + vapor	251.2	2.385	0.8069
$6H_2O$ + $2H_2O$ + solution + vapor	334.6	5.519	0.5527
$6H_2O$ + $1H_2O$ + solution + vapor[(1)]	342.5	6.851	0.4793
$2H_2O$ + $1H_2O$ + solution + vapor	405.3	7.907	0.5193
$1H_2O$ + $SrCl_2$ + solution + vapor	503.1	12.70	0.5186

(1) Metastable assembly.

with $q_1 = -6.7891$, $q_2 = 8.6424E+02$ and $q_3 = 1.4086E+01$. The calculated dissociation humidities are also shown in Fig. 4. They are considered as a reasonable estimate. At low temperature the values follow the experimental data of Hüttig and Slonim [96] (black diamonds in Fig. 4), at high temperature they are largely based on solubility data accepting the solubilities of $SrCl_2{\cdot}H_2O$ reported by Benrath [85]. Based on this approach the invariant point $SrCl_2{\cdot}H_2O$ + $SrCl_2$ + solution + vapor is modeled at 503 K (Table 7).

In lack of reliable experimental data a safe prediction about the stable existence of $SrCl_2{\cdot}0.5H_2O$ is not possible. Following Lutz et al. [100] the existence of a small stability field of $SrCl_2{\cdot}0.5H_2O$ inserted between the stability fields of $SrCl_2{\cdot}H_2O$ and $SrCl_2$ above about 438 K may be expected.

After the final data evaluation was finished, a comprehensive review of strontium chloride solubilities by Krumgalz [102] came to the attention of the author. In general, the recommended solubilities in both studies at temperatures below 400 K are in reasonable agreement. The deviations below 275 K result from the fact that Krumgalz [102] did not consider the low temperature solubilities of Tenu and Counioux [43] that were the main source of data in the present evaluation. At high temperatures (>400 K), however, there are significant deviations. In the present study, the transition temperature for the $SrCl_2{\cdot}2H_2O$–$SrCl_2{\cdot}H_2O$ transition is modeled at 405 K which is in good agreement with solubilities reported by Menzies [82] and with the dissociation humidities reported by Collins and Menzies [67]. In contrast, the solubilities of $SrCl_2{\cdot}2H_2O$ recommended by Krumgalz [102] at temperatures above 405 K are largely based on data of Benrath [85], which were rejected in the present work. This leads to a transition temperature at 439 K, which is inconsistent with other experimental data.

Krumgalz [102] also calculated solubility products of the strontium chloride hydrates using ion interaction parameters valid at 298.15 K as tabulated by Pitzer [12]. The calculation of the parameters at other temperatures by extrapolation is based on temperature derivatives at 298.15 K also tabulated by Pitzer [12]. However, the temperature derivatives for $SrCl_2$(aq) are only valid to 0.1 mol kg^{-1} [12] thus, large errors are expected at temperatures far from 298.15 K. In fact, the activity coefficients and water activities of the saturated solutions and the resulting solubility products tabulated by Krumgalz [102] are in good agreement with the present model at 298.15 K but are significantly in error at other temperatures.

3.4. Implications for thermochemical heat storage

In heat storage applications salt hydrates are charged by heat induced dehydration of a higher hydrated state according to the forward reaction in Eq. (4). Thus, heat is stored in the lower hydrated state which is a stable state as long as the salt is kept dry. This offers, in comparison to other storage technologies, the major advantage of nearly loss-free heat storage over long periods of time, e.g. for seasonal storage of solar thermal energy. During discharge, heat is released as the heat of reaction of the hydration back-reaction. The enthalpy of reaction per mole of salt, $\Delta_{hyd}H$, for the hydration reaction is given by

$$\Delta_{hyd}H_{B-A} = \Delta_f H_{SrCl_2 \cdot n_A H_2O(cr)} - \Delta_f H_{SrCl_2 \cdot n_B H_2O(cr)} - (n_A - n_B)\Delta_f H_{H_2O(g)} \quad (12)$$

where $\Delta_f H$ are the enthalpies of formation of H_2O(g) and of the crystal hydrates. With $\Delta_f H_{H_2O(g)} = -241.83$ kJ mol^{-1} [61] and the enthalpies of formation of the $SrCl_2$ hydrates taken from Wagman et al. [103], this yields $\Delta_{hyd}H_{0-6} = -342.9$ kJ mol^{-1} for the hydration of the anhydrous salt and formation of $SrCl_2{\cdot}6H_2O$ at 25 °C. The corresponding enthalpy of hydration per mole H_2O is $\Delta_{hyd}H_0 = \Delta_{hyd}H/(n_A - n_B) = -57.2$ kJ mol^{-1}. A major advantage of thermochemical storage with salt hydrates is the very high energy density, i.e. the

amount of energy stored per unit volume. For the full hydration from the anhydrous salt to the hexahydrate, the theoretical storage density is $-\Delta_{hyd}H/V_{m,SrCl_2\cdot 6H_2O} = 2.51\ GJ\,m^{-3}$ where the molar volume of $SrCl_2\cdot 6H_2O$ $V_{m,SrCl_2\cdot 6H_2O}$ was calculated from the crystallographic density [104]. This is a theoretical storage density as it is based on the volume of a single crystal of $SrCl_2\cdot 6H_2O$. In a real application, the total volume of a packed bed is larger and the volumetric storage density of the material is lower. Nonetheless, the storage density is significantly higher than typical values achieved in sensible heat storage with water or in storage with phase change materials.

Ideal storage materials not only have a high storage density but are easily dehydrated at moderate temperature, require low water vapor pressures in the hydration reaction and do not form solutions at high water vapor pressures. In other words, the stability field of the hydrated phase in the φ/T space must be as large as possible. In the case of $SrCl_2\cdot 6H_2O$, there is an absolute upper temperature limit of 335 K above which the hexahydrate is not stable any more. To make full use of the very high storage density mentioned before, it is important that this temperature is not exceeded in a reactor bed. Therefore, the heat released during the hydration reaction has to be effectively dissipated. Due to the high deliquescence humidities of all $SrCl_2$ hydrates, the formation of a solution is not expected to be critical. The water vapor pressure required for the hydration reaction should be as low as possible and is given by the $SrCl_2\cdot 6H_2O$–$SrCl_2\cdot 2H_2O$ equilibrium curve. Whether this minimum humidity is acceptable depends on the particular application, i.e. the working temperature and the availability of water vapor. For residential heating applications an acceptable upper limit of the water vapor partial pressure of (1.2–2) kPa was suggested [9,105]. These limiting isobars are shown in Fig. 5. They result in an upper temperature limit of (299–307) K above which the hexahydrate state cannot be reached at the respective water vapor pressures (points A and B in Fig. 5). These temperatures are not sufficient for the production of hot tap water and may also be inappropriate as fluid temperatures in underfloor heating systems. Thus, making use of the complete hydration to the hexahydrate state to achieve the maximum storage density requires higher water vapor pressures.

If the state of the hexahydrate cannot be reached, the dihydrate is the next-highest state of hydration. In this case, the absolute temperature limit increases to 405 K and the temperature limit for hydration at (1.2–2) kPa shifts to (321–329) K (points C and D). These temperatures are considered acceptable values in residential heating applications though they are still too low for the production of hot tap water. The storage density for the hydration of the anhydrous salt to the dihydrate, calculated from the enthalpies of formation [61,103] and the crystal density of $SrCl_2\cdot 2H_2O$ [106], is 1.7 GJ m^{-3} which is still excellent compared to other storage technologies. To achieve even higher temperatures requires either higher water vapor pressures to reach the state of the dihydrate, or, the transition $SrCl_2$–$SrCl_2\cdot H_2O$ has to be used. Using the monohydrate, temperatures of about 375 K can be reached even at vapor pressures of only (1.2–2) kPa. In this case, however, the storage density calculated with the heats of formation and the crystal density of $SrCl_2\cdot H_2O$ [107] drops to 1.1 GJ m^{-3}. The $SrCl_2$–$SrCl_2\cdot H_2O$ transition may be also used in high temperature applications, e.g. storage of industrial waste heat. In this case, however, the use of an open storage system is limited to maximum temperatures of about 433 K as limited by the 0.1 MPa isobar (Fig. 5). In a closed system higher temperatures may be realized though.

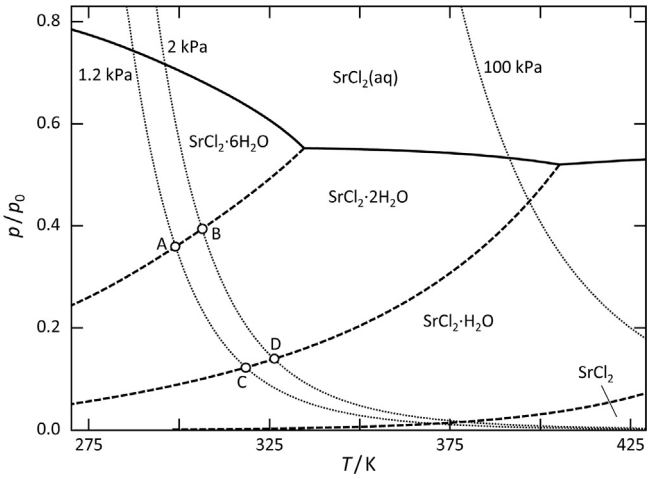

Fig. 5. Detail of the humidity–temperature phase diagram. Solid and dashed lines represent deliquescence humidities and hydration equilibria, respectively, of $SrCl_2\cdot 6H_2O$, $SrCl_2\cdot 2H_2O$ and $SrCl_2\cdot H_2O$; dotted lines represent water vapor pressure isobars at 1.2 kPa, 2 kPa and 100 kPa.

4. Conclusions

The Pitzer ion interaction model provides an accurate representation of the thermodynamic properties of aqueous $SrCl_2$(aq) over wide ranges of temperature and concentration at 0.1 MPa or saturation pressure, whichever is larger. Most of the experimental data are represented to within expected experimental uncertainties. However, there is a lack of data at high temperatures and high concentrations. The model is less well constrained and the calculated activities are less reliable above about 423 K. As the thermodynamic solubility product of $SrCl_2\cdot H_2O$ was calculated from experimental data using the present model equations, possible deviations of the predicted model activities may, at least, partially be compensated such that solubilities are still calculated accurately. The combination of solubility data with data from dissociation equilibria of $SrCl_2$ hydrates allowed for the calculation of internally consistent thermodynamic solubility products. With all data combined, the complete phase diagram involving $SrCl_2\cdot H_2O$, $SrCl_2\cdot 2H_2O$ and $SrCl_2\cdot 6H_2O$ was established. Due to a lack of experimental data, it remains uncertain whether the hemihydrate is also a stable solid in the $SrCl_2$–H_2O system. A small stability field of $SrCl_2\cdot 0.5H_2O$ at high temperature (above about 438 K) may be expected. In conclusion, additional experimental data for both concentrated solutions and the $SrCl_2$–$SrCl_2\cdot H_2O$ dissociation equilibrium at high temperature are desirable.

Strontium chloride is a promising candidate for thermochemical heat storage. Though, in comparison to other chlorides, e.g. magnesium and calcium chloride, higher vapor pressures are required for the formation of the hexahydrate, strontium chloride offers the advantage of a significantly higher deliquescence humidity. In contrast, magnesium and calcium chlorides are very deliquescent and problems with the formation of solutions during hydration were reported [108,109]. In comparison to several sulfates that were investigated recently [23,63,110,111], strontium chloride offers the advantage that lower vapor pressures are required to reach the final hydration state, i.e. the hexahydrate. Moreover, it was found by several authors that the hydration of many sulfates is sluggish which often results in incomplete hydration [112–116]. The first results of an extensive investigation on the kinetics of hydration and dehydration of $SrCl_2$ hydrates are promising and a detailed reported on this research will be provided elsewhere.

Acknowledgements

This research was funded by the Bundesministerium für Bildung und Forschung, Germany (BMBF, Grant No. 03EK3019A).

The author thanks Prof. Wolfgang Voigt and an anonymous reviewer for carefully reading the manuscript and constructive comments.

References

[1] W. Kessling, E. Laevemann, M. Peltzer, Int. J. Refrig. 21 (1998) 150–156.
[2] M. Sahlot, S.B. Riffat, Int. J. Low-Carbon Technol. 11 (2016) 489–505.
[3] A. Lowenstein, Sci. Technol. Built Environ. 14 (2008) 819–838.
[4] L. Scapino, H.A. Zondag, J. Van Bael, J. Diriken, C.C.M. Rindt, Appl. Energy 190 (2016) 920–948.
[5] W. Voigt, D. Zeng, Pure Appl. Chem. 74 (2002) 1909–1920.
[6] B. Zalba, J.M. Marín, L.F. Cabeza, H. Mehling, Appl. Therm. Eng. 23 (2003) 251–283.
[7] M.M. Farid, A.M. Khudair, S.A.K. Razack, S. Al-Hallaj, Energy Convers. Manage. 45 (2004) 1597–1615.
[8] L.G. Gordeeva, Yu.I. Aristov, Int. J. Low-Carbon Technol. 7 (2012) 288–302.
[9] P.A.J. Donkers, L.C. Sögütoglu, H.P. Huinink, H.R. Fischer, O.C.G. Adan, Appl. Energy 199 (2017) 45–68.
[10] Z. Iyimen-Schwarz, M.D. Lechner, Thermochim. Acta 68 (1983) 349–361.
[11] B. Carlsson, Sol. Energy 83 (2009) 485–500.
[12] K.S. Pitzer, in: Activity Coefficients in Electrolyte Solutions, CRC Press, Boca Raton, 1991, pp. 75–153.
[13] R.C. Phutela, K.S. Pitzer, P.P.S. Saluja, J. Chem. Eng. Data 32 (1987) 76–80.
[14] K.S. Pitzer, P. Wang, J.A. Rard, S.L. Clegg, J. Solution Chem. 28 (1999) 265–282.
[15] H.F. Holmes, R.E. Mesmer, J. Chem. Thermodyn. 28 (1996) 1325–1358.
[16] S.L. Clegg, J.A. Rard, D.G. Miller, J. Chem. Eng. Data 50 (2005) 1162–1170.
[17] R. Beyer, M. Steiger, J. Chem. Thermodyn. 34 (2002) 1057–1071.
[18] R. Beyer, M. Steiger, J. Chem. Eng. Data 55 (2010) 830–838.
[19] J. Dorn, M. Steiger, J. Chem. Eng. Data 52 (2007) 1785–1790.
[20] M. Steiger, Chem. Geol. 436 (2016) 84–97.
[21] J.A. Rard, R.F. Platford, in: Activity Coefficients in Electrolyte Solutions, CRC Press, Boca Raton, 1991, pp. 209–277.
[22] A. Lassin, J. Duplay, O. Touret, Y. Tardy, C.R. Acad. Sci. Paris Ser. A 333 (2000) 533–540.
[23] M. Steiger, K. Linnow, D. Ehrhardt, M. Rohde, Geochim. Cosmochim. Acta 75 (2011) 3600–3626.
[24] R.A. Robinson, Trans. Faraday Soc. 36 (1940) 735–738.
[25] R.H. Stokes, Trans. Faraday Soc. 44 (1948) 295–307.
[26] C.J. Downes, J. Chem. Thermodyn. 6 (1974) 317–323.
[27] J.B. Macaskill, D.R. White, R.A. Robinson, R.G. Bates, J. Solution Chem. 7 (1978) 339–347.
[28] J.A. Rard, D.G. Miller, J. Chem. Eng. Data 27 (1982) 169–173.
[29] L. Guo, B. Sun, D. Zeng, Y. Yao, H. Ha, J. Chem. Eng. Data 57 (2012) 817–827.
[30] D.G. Archer, J. Phys. Chem. Ref. Data 21 (1992) 793–821.
[31] D.G. Archer, J. Phys. Chem. Ref. Data 28 (1999) 1–18.
[32] J.A. Rard, S.L. Clegg, J. Chem. Eng. Data 42 (1997) 819–849.
[33] H.F. Holmes, R.E. Mesmer, J. Chem. Thermodyn. 13 (1981) 1025–1033.
[34] J.R.I. Hepburn, J. Chem. Soc. (1932) 550–566.
[35] K.R. Patil, A.D. Tripathi, P. Gopal, S.S. Katti, J. Chem. Eng. Data 36 (1991) 225–230.
[36] F. Rüdorff, Ann. Phys. 221 (1872) 599–622.
[37] M. de Coppet, Ann. Chim. Phys. (1872) 502–553.
[38] E.H. Loomis, Phys. Rev. 4 (1897) 273–296.
[39] H.C. Jones, F.H. Getman, Am. Chem. J. 27 (1902) 433–444.
[40] H.C. Jones, J.N. Pearce, Am. Chem. J. 38 (1907) 683–743.
[41] H.C. Jones, C.M. Stine, Am. Chem. J. 39 (1908) 313–402.
[42] O. Klein, O. Svanberg, Medd. K. Vetenskapsakademiens Nobelinstitut, Almqvist & Wiksells Boktryckeri AB, Stockholm 4 (1918) 1–13.
[43] R. Tenu, J.J. Counioux, J. Chem. Res. (M) (1990) 2453–2473.
[44] I.M. Klotz, R.M. Rosenberg, Chemical Thermodynamics, Basic Theory and Methods, 3rd ed., Menlo Park CA, Benjamin/Cunnings, 1972, pp. 374–378.
[45] J. Timmermans, The Physico-chemical Constants of Binary Systems in Concentrated Solutions. Volume 3. Systems with Metallic Compounds, Interscience Publishers, New York, 1960.
[46] G. Baroni, Gazz. Chim. Ital. 23 (1893) 249–291.
[47] R.N. Goldberg, R.L. Nuttall, J. Phys. Chem. Ref. Data 7 (1978) 263–310.
[48] W.W. Lucasse, J. Am. Chem. Soc. 47 (1925) 743–754.
[49] P. Longhi, T. Mussini, E. Vaghi, J. Chem. Thermodyn. 7 (1975) 767–776.
[50] H.S. Harned, in: The structure of electrolyte solutions, John Wiley & Sons, Inc., Chapman & Hall, limited, New York, London, 1959, pp. 152–159.
[51] F.R. Pratt, J. Franklin Inst. 185 (1918) 663–695.
[52] A.E. Stearn, G.McP. Smith, J. Am. Chem. Soc. 42 (1920) 18–32.
[53] E. Lange, H. Streeck, Z. Phys, Chem. 152 (1931) 1–23.
[54] W.H. Leung, F.J. Millero, J. Chem. Thermodyn. 7 (1975) 1067–1078.
[55] K.P. Mishchenko, A. Stagis, Zh. Obshch, Khim. 40 (1970) 2537–2541.
[56] A.F. Kapustinsky, I.P. Dezideriyeva, Trans. Faraday Soc. 42 (1946) 69–77.
[57] M.K. Karapet'yants, V.A. Vasilev, N.V. Fedyainov, Russ. J. Phys. Chem. 44 (1970) 1028–1029.
[58] G. Perron, J.E. Desnoyers, F.J. Millero, Can. J. Chem. 52 (1974) 3738–3741.
[59] J.E. Desnoyers, C. de Visser, G. Perron, P. Picker, J. Solution Chem. 5 (1976) 605–616.
[60] P.P.S. Saluja, J.C. LeBlanc, J. Chem. Eng. Data 32 (1987) 72–76.
[61] W. Wagner, A. Pruß, J. Phys. Chem. Ref. Data 31 (2002) 387–535.
[62] G.S. Kell, J. Chem. Eng. Data 20 (1975) 97–105.
[63] F. Höffler, M. Steiger, Chem. Monthly (accepted manuscript), DOI: 10.1007/s00706-017-2068-8
[64] C.M. Criss, F.J. Millero, J. Solution Chem. 28 (1999) 849–864.
[65] H. Lescoeur, Ann. Chim. Phys. 19 (1890) 533–556.
[66] M. Diesnis, Bull. Soc. Chim. 2 (1935) 1901–1907.
[67] E.M. Collins, A.W.C. Menzies, J. Phys. Chem. 40 (1935) 379–397.
[68] R.H. Stokes, R.A. Robinson, Ind. Eng. Chem. 41 (1949) 2013.
[69] L.B. Rockland, Anal. Chem. 32 (1960) 1375–1376.
[70] D.T. Acheson, in: Humidity and moisture. Measurement and control in science and industry. Vol 3: Fundamentals and standards, Reinhold Publishing, New York, 1965, pp. 521–530.
[71] A.N. Kirgintsev, A.V. Luk'yanov, Russ. J. Inorg. Chem. 12 (1967) 1070–1072.
[72] B. Bergthorsson, Acta Chem. Scand. 24 (1970) 1735–1743.
[73] M.L. Pollio, D. Kitic, S.L. Resnik, Lebensm.-Wiss. Technol. 29 (1996) 376–378.
[74] V. Morillon, F. Debeufort, J. Jose, J.F. Tharrault, M. Capelle, G. Blond, A. Voilley, Fluid Phase Equilib. 155 (1999) 297–309.
[75] D.G. Archer, P. Wang, J. Phys. Chem. Ref. Data 19 (1990) 371–411.
[76] M. Steiger, J. Kiekbusch, A. Nicolai, Construct. Build. Mater. 22 (2008) 1841–1850.
[77] P. Kremers, Ann. Phys. 168 (1854) 497–520.
[78] G. Mulder, Scheikundige Verhandelingen en Onderzoekingen 3 (3) (1864) 116–119.
[79] W.A. Tilden, J. Chem. Soc. 45 (1884) 266–270.
[80] M. Etard, Ann. Chim. Phys. 7. Sér. 2 (1894) 503–574.
[81] W.F. Ehret, J. Am. Chem. Soc. 54 (1932) 3126–3134.
[82] A.W.C. Menzies, J. Am. Chem. Soc. 58 (1936) 934–937.
[83] F.T. Miles, A.W.C. Menzies, J. Am. Chem. Soc. 59 (1937) 2392–2395.
[84] H. Bassett, H.F. Gordon, J.H. Henshall, J. Chem. Soc. 56 (1937) 971–973.
[85] A. Benrath, Z. Anorg, Allg. Chem. 247 (1941) 147–160.
[86] G.O. Assarsson, J. Phys. Chem. 57 (1953) 207–210.
[87] G.O. Assarsson, J. Phys. Chem. 57 (1953) 717–727.
[88] M.A. Clynne, R.W. Potter, J. Chem. Eng. Data 24 (1979) 338–340.
[89] Y.-J. Bi, B. Sun, J. Zhao, P.-S. Song, W. Li, Chin. J. Inorg. Chem. 27 (2011) 1765–1771.
[90] X. Zhang, S.-H. Sang, S.-Y. Zhonga, W.-Y. Huanga, Russ. J. Phys. Chem. 89 (2015) 2322–2326.
[91] D. Li, S. Sang, R. Cui, C. Wei, J. Chem. Eng. Data 60 (2015) 1227–1232.
[92] A.H. Pareau, Ann. Phys. Chem. 237 (1877) 39–63.
[93] P.C.F. Frowein, Z. Phys, Chem. 1 (1877) 5–14.
[94] M.H. Lescoeur, Ann. Chim. Phys. 6. Sér. 19 (1890) 533–556.
[95] G.P. Baxter, J.E. Lansing, J. Am. Chem. Soc. 42 (1920) 419–426.
[96] G.F. Hüttig, C. Slonim, Z. Anorg, Allg. Chem. 185 (1929) 65–77.
[97] J. Bell, J. Chem. Soc. (1937) 459–461.
[98] J.-J. Kessis, C.R. Acad, Sci. Paris C 264 (1967) 2141–2143.
[99] W.W. Wendlandt, Thermochim. Acta 12 (1975) 359–366.
[100] H.D. Lutz, B. Frischemeier, Ch. Mertins, W. Becker, Z. Anorg, Allg. Chem. 441 (1978) 205–212.
[101] T.W. Richards, V. Yngwe, J. Am. Chem. Soc. 40 (1918) 89–95.
[102] B.S. Krumgalz, J. Phys. Chem. Ref. Data 46 (2017) 043101.
[103] D.D. Wagman, W.H. Evans, V.B. Parker, R.H. Schumm, I. Halow, S.M. Bailey, K. L. Churney, R.L. Nuttal, J. Phys. Chem. Ref. Data 11 (Suppl. 2) (1982) 1–392.
[104] R.B. English, L.R. Nassimbeni, Acta Cryst. C 40 (1984) 580–581.
[105] K.E. N'Tsoukpoe, T. Schmidt, H.U. Rammelberg, B.A. Watts, W.K.L. Ruck, Appl. Energy 124 (2014) 1–16.
[106] H.E. Swanson, H.F. McMurdie, M.C. Morris, E.H. Evans, B.A.T. Paretzkin, Standard X-ray diffraction powder patterns. Section 11 – Data for 70 substances, National Bureau of Standards Monograph 25, U.S. Government Printing Office, Washington D.C. (1974) p. 58.
[107] A. Haase, G. Brauer, Z. Anorg, Allg. Chem. 450 (1979) 36–44.
[108] V.M. van Essen, J. Cot Gores, L.P.J. Bleijendaal, H.A. Zondag, R. Schuitema, M. Bakker, W.G.J. van Helden, Proceedings 3rd International Conference of Energy Sustainability, ASME, San Francisco, 2009.
[109] C.J. Ferchaud, H.A. Zondag, J.B.J. Veldhuis, R. de Boer, J. Phys. Conf. Ser. 395 (2012) 012069.
[110] F. Höffler, M. Steiger, J. Chem. Thermodyn. 116 (2018) 279–288.
[111] K. Posern, K. Linnow, M. Niermann, Ch. Kaps, M. Steiger, Thermochim. Acta 611 (2015) 1–9.
[112] K. Posern, Ch. Kaps, J. Therm. Anal. Calorim. 92 (2008) 905–909.
[113] M. Steiger, K. Linnow, H. Juling, G. Gülker, A.E. Jarad, S. Brüggerhoff, D. Kirchner, Cryst. Growth. Des. 8 (2008) 336–343.
[114] V.M. van Essen, H.A. Zondag, J.C. Gores, L.P.J. Bleijendaal, M. Bakker, R. Schuitema, W.G.J. van Helden, Z. He, C.C.M. Rindt, J. Sol. Energy Eng. 131 (2009) 041014.
[115] K. Linnow, M. Niermann, P. Bonatz, K. Posern, M. Steiger, Energy Proced. 48 (2014) 394–404.
[116] P.A.J. Donkers, L. Pel, O.C.G. Adan, J. Energy Stor. 5 (2016) 25–32.